Published in final edited form as:
Magn Reson Med. 2010 February ; 63(2): 349–355. doi:10.1002/mrm.22202.

Improved SNR in Phase Contrast Velocimetry with 5-Point Balanced Flow Encoding

Kevin M Johnson, Ph.D.[1] and **Michael Markl, Ph. D.**[2]

[1]Department of Medical Physics, University of Wisconsin, Madison, WI, USA

[2]Department of Diagnostic Radiology, Medical Physics, University Hospital Freiburg, Freiburg, Germany

Abstract

Phase Contrast (PC) velocimetry can be utilized to measure complex flow for both quantitative and qualitative assessment of vascular hemodynamics. However, PC requires that a maximum measurable velocity be set that balances noise and phase aliasing. To efficiently reduce noise in PC images, several investigators have proposed extended velocity encoding schemes that use extra encodings to unwrap phase aliasing; however, existing techniques can lead to significant increases in echo and scan time limiting there clinical benefits. In this work, we have developed a novel 5-point velocity encoding scheme that efficiently reduces noise with minimal increases in scan and echo time. Investigations were performed in phantoms demonstrating a 63% increase in velocity to noise ratio (VNR) compared to standard 4-point encoding schemes. Aortic velocity measurements were performed in healthy volunteers, showing similar VNR improvements. In those volunteers, it was also demonstrated that without sacrificing accuracy low resolution images can be used for the 5th encoding point reducing the scan time penalty from 25% down to less than 1%.

Introduction

Magnetic Resonance (MR) imaging can be utilized to measure three directional velocities in three dimensions using gradients to impart phase to moving spins. This unique ability has allowed the use of MR for both qualitative and quantitative assessment of complex cardiovascular hemodynamics using three dimensional, three directional, cardiac gated acquisitions (CINE) phase contrast (PC) sequences (1-7). Since MR-signal phase is only measurable from $-\pi$ to π, velocities can only be uniquely encoded up to a maximum measurable velocity (V_{enc}). Velocity sensitivity can be controlled by changing the gradients used for velocity encoding; however there is a tradeoff between noise performance and increased V_{enc}.. With 3D acquisitions setting the optimal V_{enc} is particularly challenging. Acquisition durations often exceed 10 minutes producing 1000's of images making it both impractical to repeat acquisitions and time consuming to identify aliasing from source images. Thus, often the V_{enc} must be set conservatively high leading to unnecessarily increased noise in the velocity images.

As an alternative to using a high V_{enc}, measurement with a low V_{enc} in combination with phase unwrapping can be performed to reduce phase aliasing in final velocity images. This can be done manually, however this is time consuming in nature and not practical for 3D

Corresponding Address: Kevin Johnson University of Wisconsin – Madison Department of MR/CT Research, Room #1169 Wisconsin Institutes for Medical Research (WIMR) 1111 Highland Ave. Madison, WI 53705-2275 Phone: 608 – 628 – 7351 Fax: 608 - 265-9840 kmjohnson3@wisc.edu.

applications. Automatic unwrapping algorithms have been developed that exploit the smoothness of velocity images both in space and time (8-12). These algorithms can reduce a small number of phase unwraps in certain situations; however, successful unwrapping is not guaranteed and often fails in situations of large aliased regions or multiple wrappings.

To provide more reliable phase unwrapping, investigators have proposed to add additional velocity encoding steps to standard acquisitions (13). These techniques utilize an acquisition with a high V_{enc} as a velocity estimate to unwrap the phase in a low V_{enc} acquisition. These techniques can be combined with spatial and temporal unwrapping algorithms and offer improved performance over phase unwrapping alone (10,14). However, multi-V_{enc} acquisitions require significant increases in scan time, adding at least 75% scan time for three directional encoding. Additionally, the larger flow encoding gradients required for multiple V_{enc}'s often lead to intra-voxel dephasing, which can result in reduced accuracy or VNR efficiency (15).

With multi directional velocity encoding, there is substantial freedom in the velocity encoding scheme. Instead of separate high and low V_{enc} acquisitions, an encoding scheme to measure velocities can be designed with any number of encoding points greater than the number of velocity directions. In this work, we aim to design a three directional velocity encoding scheme that utilizes 5 encoding points for improving velocity to noise ratio (VNR) efficiency. The proposed method is a practical compromise between VNR gain and intra-voxel dephasing and acquisition time increase. Additionally, this scheme can be highly accelerated using low resolution images for one of the encoding points. The new 5-point encoding strategy is investigated in phantom experiments to characterize noise and aliasing performance and initial results are shown for human volunteers.

Theory

Signal Model and Aliasing

Gradient velocity encoding is assumed to cause a phase evolution of moving spins in proportion to the velocity. In phase contrast, the signal, S, from a given voxel is described:

$$S\left(\vec{M}_1\right)=\rho e^{i\vec{v}\bullet\gamma\vec{M}_1+\theta} \quad 1$$

where $\vec{M}_1$ is the first moment of the gradients at echo time, γ is the gyromagnetic ratio, ρ is the signal intensity, $\vec{v}$ is the velocity, and θ is a phase offset. For three directional flow encoding, at least four measurements are made with different values of $\vec{M}_1$. To prevent errors from phase offsets, a reference direction is chosen and the signal from each encoding is multiplied by the complex conjugate of the signal from the reference direction (16). The resulting signal is described:

$$S_j=\rho^2 e^{i\vec{v}\bullet\gamma\Delta\vec{M}_1} \quad 2$$

where j is the encoding number, ΔM_1 is the difference in first moment from the velocity encoding of interest to the reference position. Subsequently the phase is taken and arranged in set of linear equations. Written in matrix notation:

$$\phi=Av \quad 3$$

where A is a matrix containing the $\gamma\Delta M_1$ values for each encoding in rows, v is the column vector of velocities, and ϕ is the vector of measured phase differences. The least squared solution to Equation 3 is computed using a Moore-Penrose pseudo inverse of A, A^+. Since

the phase can only be uniquely measured from $-\pi$ to $+\pi$, the aliasing free space is defined as the 3D space spanned by the 3 velocity components where all values of ϕ are within $-\pi$ to $+\pi$. The minimum velocity magnitude over all directions that results in a phase magnitude greater than π is defined as the V_{enc}. The V_{enc} can be computed directly from Equation 3:

$$V_{enc}=\pi \cdot \min\left(\sum_{k=1}^{3} A_{j,k}^{2}\right)^{-\frac{1}{2}} \quad 4$$

where k is the velocity direction and min is the minimum over all velocity encodings.

Encoding Schemes

For the three directional flow encoding situation, two common choices for flow encoding are balanced (i.e. Hadamard) (17,18) and referenced 4-point methods (19). 4-point referenced encodes three orthogonal directions independently with respect to a reference flow encoding such that A is a diagonal matrix. 4-point balanced acquisitions can be represented by 4 mutually equidistant points in M_1 space, i.e. forming a regular tetrahedron. To increase the effective V_{enc} of these encoding schemes, phase unwrapping can be performed using an estimate of the velocity, $v_{estimate}$, either from a separate acquisition, or from additional velocity encoding steps:

$$\phi_{un-aliased}=\phi+2\pi \cdot NI\left(\frac{Av_{estimate}-\phi}{2\pi}\right) \quad 5$$

where NI is the nearest integer function. This un-aliased phase can then be used solve Equation 3. Previous work has estimated the velocity using 7-point referenced encoding schemes with separate high and low V_{enc} acquisitions sharing a reference point (13) requiring 75% more scan time. Without intra-voxel velocity dispersion, the ratio of the high to low V_{enc} ratio is directly proportional to the VNR improvement over a single V_{enc} approach. However, as the high to low V_{enc} ratio is increased, the single velocity per voxel approximation breaks down leading to inaccuracies in the final velocity estimate. These inaccuracies can be resolved by identifying areas of intra-voxel dispersion and only using the high V_{enc} encodings in those regions (15). However, this nulls the VNR benefits of multi-V_{enc} encoding in those voxels and requires utilization of a flow compensated reference point.

To reduce the scan time penalty and limit inaccuracies caused by intra-voxel dispersion, we propose the utilization of a 5-point method as shown in Table 1. This encoding strategy corresponds to the balanced 4-point acquisition with an added flow-compensated measurement. This scheme is also gradient balanced with a net 1st moment of zero over the 5 TR's required for acquisition, subsequently we term it to be 5-point balanced encoding. We propose to determine a velocity estimate using the flow compensated measurement ($M_1 = 0$) as the reference acquisition in Equation 2. Subsequently the velocity is determined using only the 4 non-flow compensated acquisitions, with the phase unwrapped using Eq. 5 before solving. Written as a single step, the velocity is computed:

$$v=A_1^{+}\left(\phi_1+2\pi N.I.\left(\frac{A_1A_0^{+}\phi_0-\phi_1}{2\pi}\right)\right) \quad 6$$

where A_1 and ϕ_1 are respectively the encoding matrix and phases using only the 4 non-flow compensated encodings, A_0 and ϕ_0 are respectively the encoding matrix and phases using all 5-encodings and the flow compensated point as a reference. Since the nearest integer function effectively eliminates noise from the velocity estimate, the noise in the final

velocity is determined by A_1^+ and has the same noise properties as 4-point balanced encoding. However, since the phase aliasing is unwrapped, the velocity aliasing is determined by A_0 . Using this method, for a given V_{enc} the maximum 1st moment can be larger improving the velocity to noise ratio VNR by 62% as shown in Table 1. Relative to the commonly used 4-point referenced encoding this translates to a 15% increase in the first moment.

The maximum measurable velocity is directionally dependent for all three directional flow encoding schemes, and the shape of the aliasing space is different with the proposed 5-point scheme. 3D isosurfaces of the aliasing free space are shown in Figure 1 for 4-point balanced, 4-point referenced, and 5-point balanced acquisitions. For 4-point referenced encoding, the aliasing shape is a cube, for which aliasing occurs first along the x, y, and z directions. For the 4-point balanced acquisition, the shape is more complex with aliasing first occurring when (v_x=v_y,v_z=0), (v_x=v_z,v_y=0), or (v_y=v_z,v_x=0). For the 5-point method, the shape is more symmetric than the balanced method with aliasing occurring when (v_x=v_y=v_z), (v_x=v_y=-v_z), (v_x=-v_y=v_z), and (-v_x=v_y=v_z).

Accelerated Referenced Acquisition

The 5-point method comes at the cost of an additional measurement point, which will reduce achievable temporal resolutions and/or extend acquisition times. However, since the 5th point is only used for phase unwrapping small errors will have limited impact on the final velocity measurement. It can be acquired in separate heartbeat, removing the temporal resolution penalty. To remove the scan time penalty, the acquisition of the 5th point could also be accelerated. Previous work has shown that one-sided 2-point flow encoding can be accelerated by acquiring flow compensated reference images at low temporal and spatial resolution (20). This assumes phase offsets are temporally stable and/or spatially smooth. Subsequent errors are introduced wherever rapidly varying phase offsets occur: fat/water boundaries, susceptibility boundaries, and moving structures. In the proposed 5-point method, phase errors must induce an error in $A_1 A_0^+ \phi_0$ greater than π to have any effect. Thus, for 5-point acquisitions we hypothesize that significant reductions in the temporal and spatial resolution can be performed without compromise in velocity accuracy.

Methods

MR Experiments

All MR experiments were performed on a 3 T MRI system (Magnetom TRIO; Siemens, Erlangen, Germany; slew rate: 200 mT/m/ms, max gradient strength: 40 mT/m). 5-point flow encoding was introduced into an ecg-triggered 2D spoiled gradient echo phase contrast sequence with interleaved velocity encoding. Flow encoding gradients were designed using minimum TE calculation for both 4-point and 5-point encoding schemes (21). Initial phantom experiments were performed to verify aliasing space improvement and quantify noise performance. To identify aliasing patterns, a phantom consisting of a pneumatically powered rotating drum was imaged using standard 4-point referenced and the newly developed 5-point balanced encoding schemes. Common parameters include: FOV = 300mm, in plane resolution=1.7×1.7mm slice thickness = 4 mm, flip angle=5, V_{enc} = 50 cm/s. The 4-point referenced exam had a TE/TR of 4.6/7.3ms, while the 5-point acquisition had a TE/TR of 4.7/7.5. The slight increase in TE/TR is due to the 15% increase in required 1st moment for the 5-point exam. 5-point velocity images were reconstructed using both full 5-point processing and using only the 4-point balanced acquisition encodings. Images were visually examined to identify aliasing patterns and noise. To specifically quantify noise reduction, a pneumatically controlled translation phantom consisting of sliding Gd-doped phantom was imaged using the same sequences. Each sequence was repeated twice, and

final velocity images were subtracted to remove variations from background phase offsets. A region of interest (ROI) was drawn in the subtracted images and the standard deviation was computed and compared across encoding schemes.

To evaluate the effectiveness of 5-point encoding in-vivo and assess acceleration using low resolution images, 3 healthy volunteers were imaged with institutional review board approval and informed consent. A single slice was localized through the center of the ascending and descending aorta for 3-directional flow encoding. 2D, free-breathing, navigator gated, CINE, PC images were subsequently acquired using 5-point balanced and 4-point referenced acquisitions using an 8-channel phased array cardiac coil. Common parameters include: Resolution =1.4 mm × 1.4 mm, FOV=360, navigator window = ±5.0mm, flip angle = 15°, no k-space sharing between time frames, readout bandwidth = 450 Hz/pixel, TR=5.10ms, V_{enc}=150cm/s. 5-point exams had an insignificantly extended TE of 2.673 ms compared to the 4-point point referenced that had a TE of 2.633. Note both TE's are relatively close to 2.4 ms, the time required for a 2π phase evolution of fat. 5-point velocity images were reconstructed using both full 5-point processing and using only the 4-point balanced acquisitions. To investigate accelerated reference acquisition, the flow compensated image of the 5-point scheme was retrospectively reconstructed using a segmented k-space acquisition. The number of shared phase encoding lines ranging from 1 to 19 lines in increments of 2, each of which was reconstructed using a phase encoding resolution reduction ranging from 1 to 30. To identify aliasing automatically, we measured the phase error:

$$\left\| \left(v\left(\vec{r}\right) - v_{full}\left(\vec{r}\right) \right) \cdot M \right\|_2 \qquad 7$$

Where $v\left(\vec{r}\right)$ is the test velocity data from all volunteers, $v_{full}\left(\vec{r}\right)$ is the velocity using a full resolution flow compensated datasets from all volunteers, and M is a binary mask. The mask is calculated by thresholding the magnitude images using 10% of the maximum signal. In this way, pixels that are dominated by noise such as those in air spaces are removed from the detection of aliasing.

Results

Phantom Experiments

Figure 2 shows an example magnitude image from 5-point encoding and velocity images for the rotating phantom for 4-point balanced velocity encoding, 4-point referenced, and the proposed 5-point velocity encoding. Magnitude images show geometric distortion caused by displacement artifact that is common to all velocity encoding directions. Additionally, ghosting of the edges of the phantom occurs due to the imperfect motion of the phantom. 4-point balanced images, derived from the 4-outer points of the 5-point acquisitions, show significant velocity aliasing. The shape of the aliasing pattern strongly agrees with the theoretical shape shown in Figure 1. 5-point balanced and 4-point referenced images show no aliasing, while 5-point aliasing images visually show reduced noise. 5-point phantom noise measurements in the sliding phantom show a noise level of 9.51±1.02 cm/s, compared to 15.56±1.34 cm/s with the 4-point referenced acquisition. This represents a noise improvement of 1.636 agreeing almost exactly with the theoretical ratio of 1.633.

Volunteer Experiments

Example volunteer systolic velocity images of 4-point referenced, 5-point balanced, and 4-point balanced images are shown in Figure 3. 5-point images show significant improvements in VNR compared to 4-pt referenced encoding with the same V_{enc}. The acquisition of PC

images with 4-pt balanced encoding with the same first moments used for 5-pt encoding results in identical VNR but V_{enc} reduced by 62% (Figure 3, right columns) and therefore substantial phase aliasing. Note that aliasing in 4-point balanced velocity shows substantial dependence on the direction of velocity. This aliasing was effectively removed by the phase unwrapping procedure used for the 5-point images. Vector plots of the aortic arch during systole and during slow flow are shown in Figure 4, for both 5-point balanced and 4-point referenced encoding schemes. In systole, velocities are near the V_{enc} resulting in minimal visual difference between the encoding schemes. During flow reversal, velocities are substantially lower than the V_{enc} such that the improved VNR of 5-point encoding allows better visualization of the flow patterns. Source S/I velocity images for accelerated 5-point are shown in Figure 5a with quantified aliasing across all velocity directions and volunteers shown in Figure 5b. Insufficient unwrapping generally occurs at air-tissue interfaces where strong background phase variations are expected. Aliasing is not detected until the temporal resolution is more than 331 ms and/or the voxel size is greater than 23.8mm. At the minimum resolution without detected aliasing (331ms, 23.8mm) this represents a 0.1% increase in scan time compared to full resolution 4-point exam.

Discussion

The 5-point flow encoding scheme with phase unwrapping substantially increases VNR efficiency compared to existing techniques. We presented in-vivo results utilizing accelerated 5-point encoding capable of improving the VNR by 60% with less than a 1% increase in scan time. For the same SNR performance with signal averaging, the scan time would need to increase by at least 2.7 times. The method also represents a minimum 1^{st} moment increase, which is likely to limit intra-voxel dephasing that can be a severe drawback in other multi-point point encoding schemes.

Compared to velocity image based phase unwrapping techniques, the 5-point method is less susceptible to unwrapping errors associated with complex flow, vessel boundaries, cardiac pulsatility, and cardiac motion. Additionally, the 5-point scheme requires only minor changes to the reconstruction, with no free parameters. The 5-point method has a well defined V_{enc} and aliasing errors are well described. Errors in velocity image unwrapping techniques, based on the reduction of rapid spatial or temporal changes velocity, occur both when a starting point is difficult to identify and when sharp physiological changes in velocity are incorrectly identified as aliasing. The 5-point and image based phase unwrapping techniques are not mutually exclusive and can be combined to further improve VNR. For example, for a desired maximum measurable velocity of 150cm/s, the 5-point V_{enc} can be set to 100 cm/s for a maximum phase wrapping error of $\frac{\pi}{2}$ that can be unwrapped with velocity image based techniques. Such an approach could result in a combined VNR improvement of 2.4× (1.6× 5-point, 1.5× phase unwrapping).

The proposed 5-point encoding strategy requires less time and utilizes smaller 1^{st} moment magnitudes compared to multi-V_{enc} approaches. The scan time increase of standard multi-V_{enc} approach is at a minimum 75% of the standard 4-point method, while the 5-point method requires an increase of 1 to 25%. Given the lengthy nature of PC exams, especially in 3D applications where scan times can be greater than 10 minutes, these time savings represent a significant benefit. The reduced scan time allows for the utilization of lower first moment gradients without sacrificing VNR efficiency. To maintain the same VNR efficiency as an un-accelerated 5-point acquisition the V_{enc} ratio, F, must be at least 2.3 for a standard 7-point multi-V_{enc} encoding resulting in larger velocity encoding gradients. Larger gradients lead to errors in the unwrapped low V_{enc} velocity image as the narrow spin density assumptions of PC breakdown, as caused by partial volume effects and turbulent flow. While methods exist to identify and correct these errors in standard multi-point encoding

(15), these methods effectively nulls the VNR benefits of the multi-V_{enc} approach in voxels with errors.

The acceleration of the reference data in this work was based on low temporal and spatial resolution acquisition. The required resolution for phase unwrapping is likely to be highly dependent on the application. Chemical shift and susceptibility based off-resonance are the main sources of high resolution background phase and subsequently limit what resolutions are achievable without aliasing errors. Based on the assumption that objects are relatively stationary and blood flow introduces minimal high resolution phase into the flow-compensated images, most applications are unlikely to require any temporal resolution in the flow compensated acquisition. However, the movement of fat/water boundaries in some applications, e.g. coronary PC flow measurements, may require some temporal resolution in the flow-compensated images. The spatial resolution is similarly limited by the background phase features. Strong susceptibility variations brought on by air-tissue interfaces and metallic implants must be characterized in the low-resolution flow compensated images. Fat/water boundaries are of greater concern, as they are inherently high-resolution. However, low spatial resolution background images will lead to phase unwrapping errors at fat/water boundaries only if the TE is near the fat/water out-of-phase condition. For this work, the TE was ≈2.6 ms for 5-point exams 0.2 ms different from the in-phase TE of 2.4 ms. Subsequently the phase difference between fat and water is expected to only be ≈30° and thus much smaller than π, which will not lead directly to phase unwrapping errors.

The acceleration of 5-point encoding in this paper has been limited to 1D spatial and temporal resolution reductions; however alternative or additional methods may reduce the likelihood of phase unwrapping errors. Parallel imaging can be utilized for imaging of the 5^{th} point to improve the resolution for a given scan time, which can additionally be combined with k-t acceleration techniques for gated acquisitions (22) (23). Since the 5^{th} point does not directly influence the VNR or accuracy of the final images, increased noise and errors related to k-t assumptions are more tolerable. The same can be said for other acceleration techniques including radial undersampling (24), compressed sensing (25), and prior image constrained (26) techniques. Further work is required to investigate the utilization of these techniques for improved velocity estimates.

Conclusion

In this study, we have developed a novel, 5-point velocity encoding scheme for improved VNR efficiency over standard 4-point encoding scheme. We demonstrated the efficacy of this scheme in both phantoms and volunteers. Volunteer investigations found that low resolution imaging of the 5^{th} encoding can drastically reduce the imaging time penalty. With acceleration, a 62% improvement in VNR is achieved with less than a 1% increase in scan time.

Acknowledgments

We grateful acknowledge funding support from NIH grant 2R01HL072260-05A1 and Grant support by the Deutsche Forschungsgemeinschaft (DFG), Grant # MA 2383/4-1 and the Bundesministerium für Bildung und Forschung (BMBF), Grant # 01EV0706

References

1. Markl M, Harloff A, Bley TA, Zaitsev M, Jung B, Weigang E, Langer M, Hennig J, Frydrychowicz A. Time-resolved 3D MR velocity mapping at 3T: improved navigator-gated assessment of vascular anatomy and blood flow. J Magn Reson Imaging. 2007; 25(4):824–831. [PubMed: 17345635]

2. Kvitting JP, Ebbers T, Wigstrom L, Engvall J, Olin CL, Bolger AF. Flow patterns in the aortic root and the aorta studied with time-resolved, 3-dimensional, phase-contrast magnetic resonance imaging: implications for aortic valve-sparing surgery. J Thorac Cardiovasc Surg. 2004; 127(6): 1602–1607. [PubMed: 15173713]

3. Wigstrom L, Ebbers T, Fyrenius A, Karlsson M, Engvall J, Wranne B, Bolger AF. Particle trace visualization of intracardiac flow using time-resolved 3D phase contrast MRI. Magn Reson Med. 1999; 41(4):793–799. [PubMed: 10332856]

4. Stalder AF, Russe MF, Frydrychowicz A, Bock J, Hennig J, Markl M. Quantitative 2D and 3D phase contrast MRI: Optimized analysis of blood flow and vessel wall parameters. Magn Reson Med. 2008; 60(5):1218–1231. [PubMed: 18956416]

5. Wu SP, Ringgaard S, Pedersen EM. Three-dimensional phase contrast velocity mapping acquisition improves wall shear stress estimation in vivo. Magn Reson Imaging. 2004; 22(3):345–351. [PubMed: 15062929]

6. Tyszka JM, Laidlaw DH, Asa JW, Silverman JM. Three-dimensional, time-resolved (4D) relative pressure mapping using magnetic resonance imaging. J Magn Reson Imaging. 2000; 12(2):321–329. [PubMed: 10931596]

7. Ebbers T, Wigstrom L, Bolger AF, Engvall J, Karlsson M. Estimation of relative cardiovascular pressures using time-resolved three-dimensional phase contrast MRI. Magn Reson Med. 2001; 45(5):872–879. [PubMed: 11323814]

8. Spottiswoode BS, Zhong X, Hess AT, Kramer CM, Meintjes EM, Mayosi BM, Epstein FH. Tracking myocardial motion from cine DENSE images using spatiotemporal phase unwrapping and temporal fitting. IEEE Trans Med Imaging. 2007; 26(1):15–30. [PubMed: 17243581]

9. Yang GZ, Burger P, Kilner PJ, Karwatowski SP, Firmin DN. Dynamic range extension of cine velocity measurements using motion-registered spatiotemporal phase unwrapping. J Magn Reson Imaging. 1996; 6(3):495–502. [PubMed: 8724416]

10. Salfity MF, Huntley JM, Graves MJ, Marklund O, Cusack R, Beauregard DA. Extending the dynamic range of phase contrast magnetic resonance velocity imaging using advanced higher-dimensional phase unwrapping algorithms. J R Soc Interface. 2006; 3(8):415–427. [PubMed: 16849270]

11. Xiang QS. Temporal phase unwrapping for CINE velocity imaging. J Magn Reson Imaging. 1995; 5(5):529–534. [PubMed: 8574036]

12. Salfity MF, Ruiz PD, Huntley JM, Graves MJ, Cusack R, Beauregard DA. Branch cut surface placement for unwrapping of undersampled three-dimensional phase data: application to magnetic resonance imaging arterial flow mapping. Appl Opt. 2006; 45(12):2711–2722. [PubMed: 16633421]

13. Lee AT, Pike GB, Pelc NJ. Three-point phase-contrast velocity measurements with increased velocity-to-noise ratio. Magn Reson Med. 1995; 33(1):122–126. [PubMed: 7891526]

14. Herment A, Mousseaux E, Jolivet O, DeCesare A, Frouin F, Todd-Pokropek A, Bittoun J. Improved estimation of velocity and flow rate using regularized three-point phase-contrast velocimetry. Magn Reson Med. 2000; 44(1):122–128. [PubMed: 10893530]

15. Pipe JG. A simple measure of flow disorder and wall shear stress in phase contrast MRI. Magn Reson Med. 2003; 49(3):543–550. [PubMed: 12594758]

16. Bernstein MA, Grgic M, Brosnan TJ, Pelc NJ. Reconstructions of phase contrast, phased array multicoil data. Magn Reson Med. 1994; 32(3):330–334. [PubMed: 7984065]

17. Pelc NJ, Bernstein MA, Shimakawa A, Glover GH. Encoding strategies for three-direction phase-contrast MR imaging of flow. J Magn Reson Imaging. 1991; 1(4):405–413. [PubMed: 1790362]

18. Dumoulin CL, Souza SP, Darrow RD, Pelc NJ, Adams WJ, Ash SA. Simultaneous acquisition of phase-contrast angiograms and stationary-tissue images with Hadamard encoding of flow-induced phase shifts. J Magn Reson Imaging. 1991; 1(4):399–404. [PubMed: 1790361]

19. Conturo TE, Robinson BH. Analysis of encoding efficiency in MR imaging of velocity magnitude and direction. Magn Reson Med. 1992; 25(2):233–247. [PubMed: 1614308]

20. Lin, HY.; Ding, Y.; Chung, Y.; Raman, SV.; Simonetti, OP. Efficient Velocity Mapping by Accelerated Acquisition of Phase Refererence Data.. In proceedings of 15th Annual Meeting of ISMRM; Berlin, Germany. 2007. p. 249

21. Bernstein MA, Shimakawa A, Pelc NJ. Minimizing TE in moment-nulled or flow-encoded two- and three-dimensional gradient-echo imaging. Journal of Magnetic Resonance Imaging. 1992; 2(5):583–588. [PubMed: 1392252]

22. Jung B, Honal M, Ullmann P, Hennig J, Markl M. Highly k-t-space-accelerated phase-contrast MRI. Magn Reson Med. 2008; 60(5):1169–1177. [PubMed: 18958854]

23. Baltes C, Kozerke S, Hansen MS, Pruessmann KP, Tsao J, Boesiger P. Accelerating cine phase-contrast flow measurements using k-t BLAST and k-t SENSE. Magn Reson Med. 2005; 54(6): 1430–1438. [PubMed: 16276492]

24. Gu T, Korosec FR, Block WF, Fain SB, Turk Q, Lum D, Zhou Y, Grist TM, Haughton V, Mistretta CA. PC VIPR: a high-speed 3D phase-contrast method for flow quantification and high-resolution angiography. Am J Neuroradiol. 2005; 26(4):743–749. [PubMed: 15814915]

25. Lustig M, Donoho D, Pauly JM. Sparse MRI: The application of compressed sensing for rapid MR imaging. Magn Reson Med. 2007; 58(6):1182–1195. [PubMed: 17969013]

26. Mistretta CA, Wieben O, Velikina J, Block W, Perry J, Wu Y, Johnson K, Wu Y. Highly constrained backprojection for time-resolved MRI. Magn Reson Med. 2006; 55(1):30–40. [PubMed: 16342275]

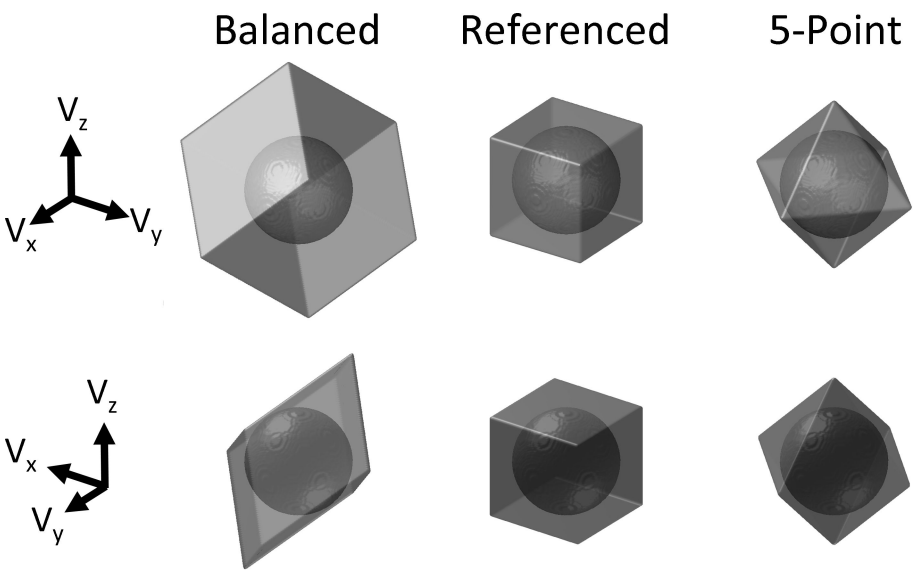

Figure 1.
Volume rendered aliasing spaces for 4-point balanced, 4-point referenced, and 5-point balanced encoding schemes viewed from 45° and -45° in the xy plane. Each shaded region has sphere rendered at the set V_{enc}. In certain directions, all methods can measure velocities higher than the prescribed V_{enc}, which is dependent on the encoding scheme. 4-point balanced encoding is particularly dependent on the velocity direction due to the rhombohedron shape, especially when compared to the cube and regular octahedron shapes of the 4-point referenced and 5-point balanced techniques, respectively.

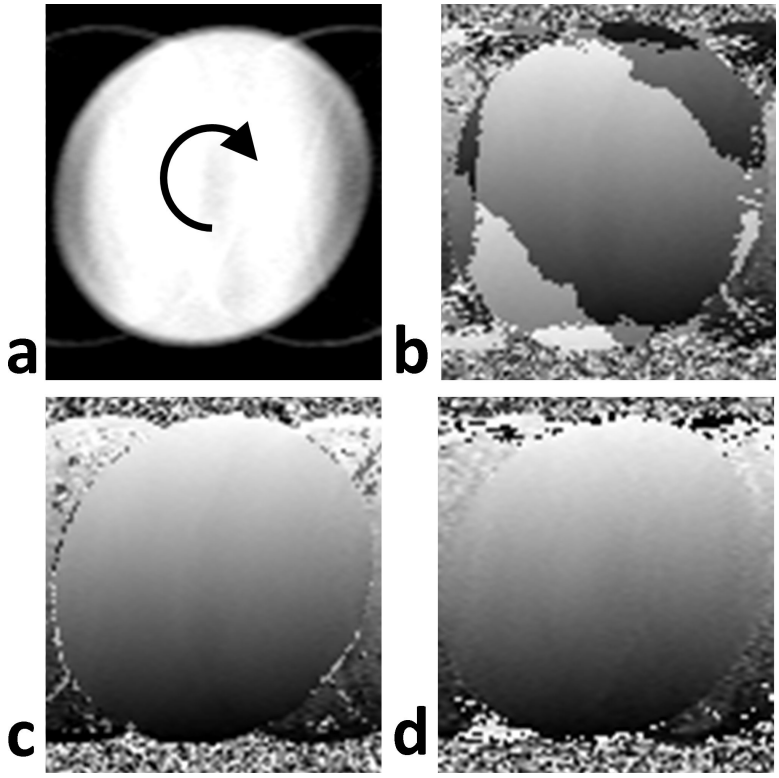

Figure 2.
Magnitude image showing phantom rotation (a) and corresponding left to right velocity images. 4-point balanced images (b) have the same first moment magnitude as the proposed 5-point scheme (c), while 4-point referenced images (d) have the same Venc as the 5-point exam. 4-point balanced images show significant aliasing, which is not evident in 5-point images. Visually, 5-point velocity images show improved VNR over 4-point referenced images.

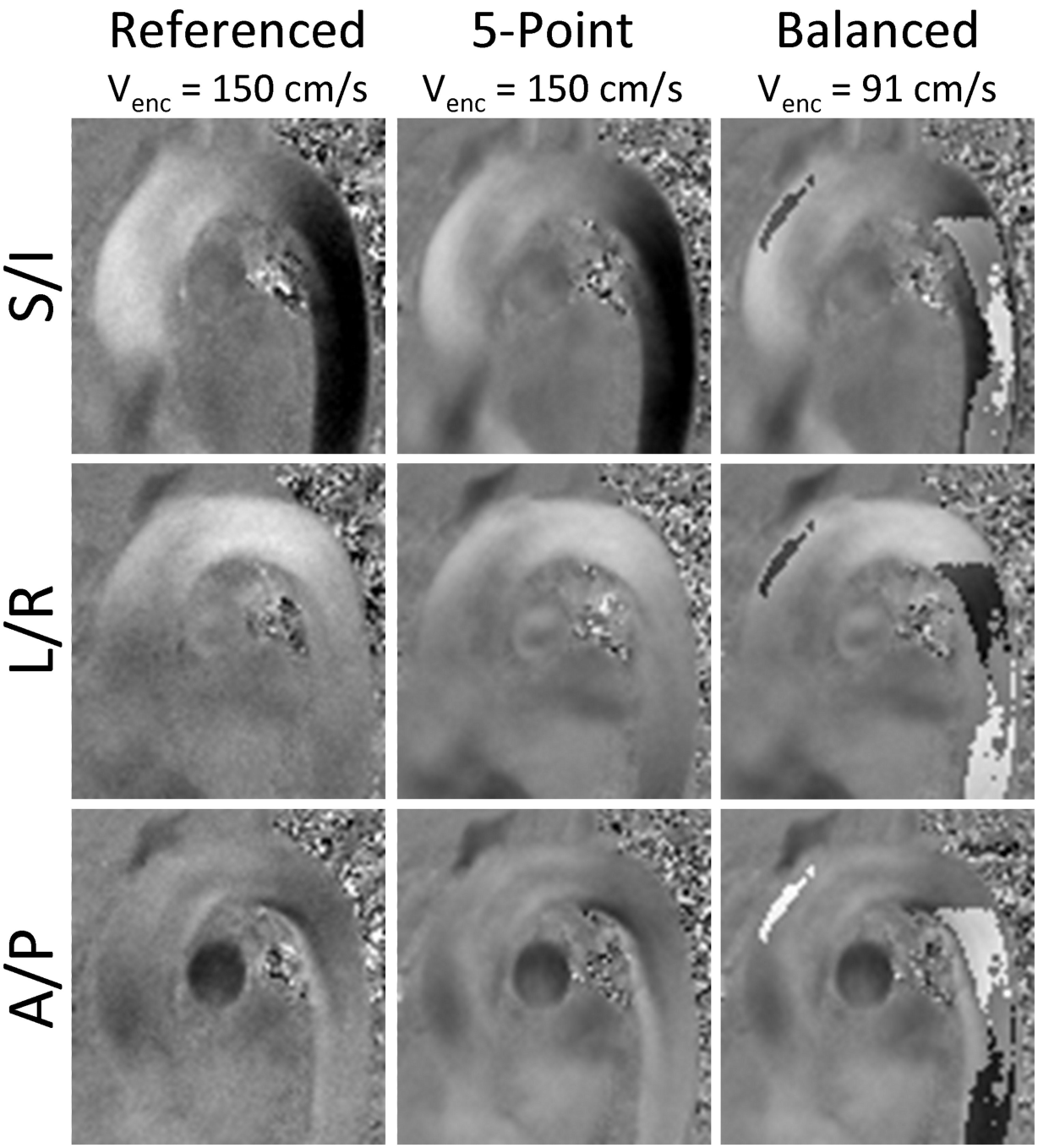

Figure 3.
Source velocity images from 4-point referenced, 4-point balanced, and 5-point acquisitions. Images from the 5-point exam show reduced noise compared to the equal V_{enc} exam (Referenced) and less velocity aliasing than the same first moment exam (Balanced).

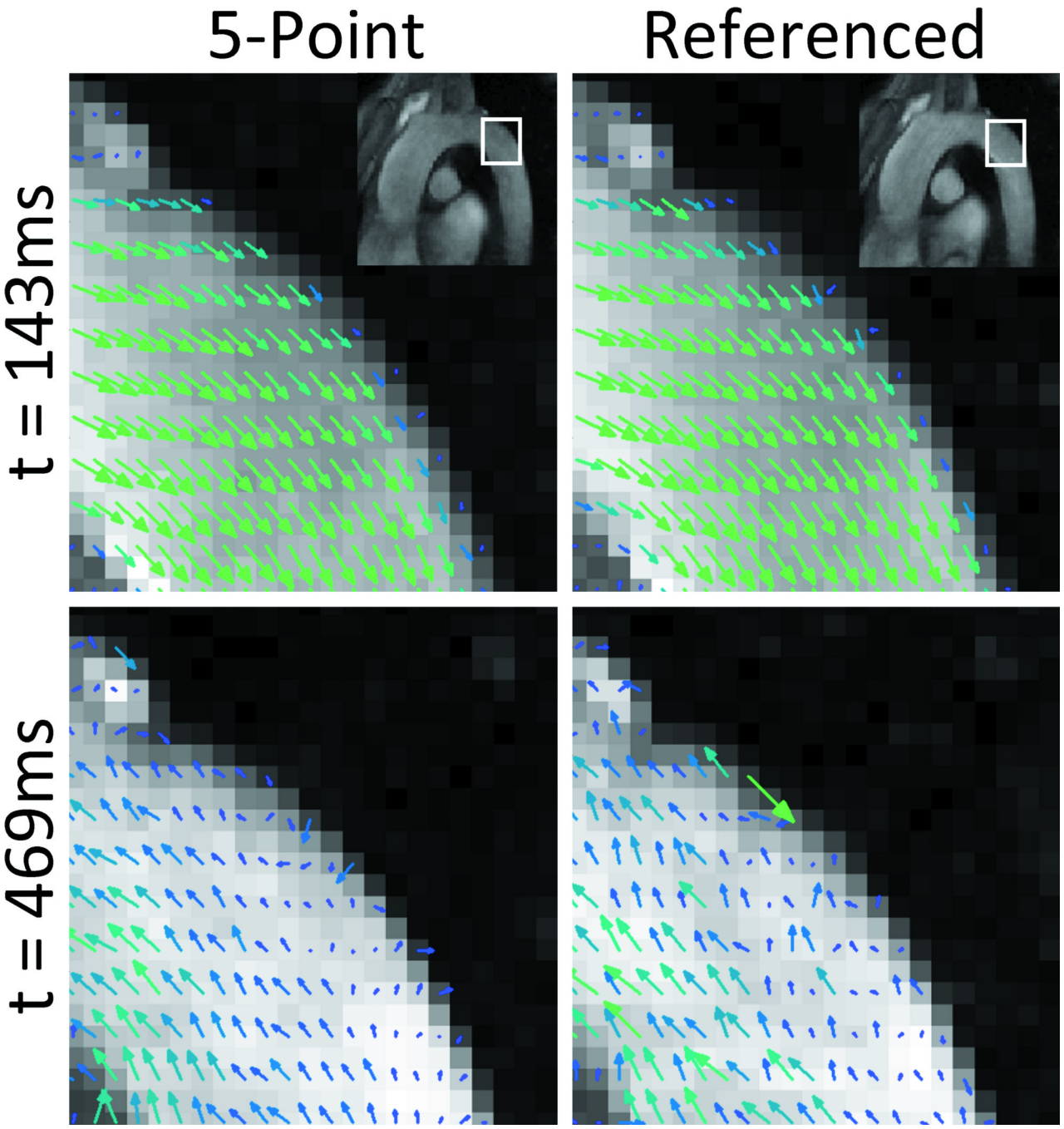

Figure 4.
In-plane vector plots during systole (t=143ms) and during peak flow reversal (t=469ms) for 5-point balanced encoding and 4-point referenced encoding. Systole images show the location of vector plots on the magnitude images. During systole, both encoding schemes produce visually similar images. During diastole, where there velocities are substantially lower, 5-point encoding shows substantially reduced noise for better visualization.

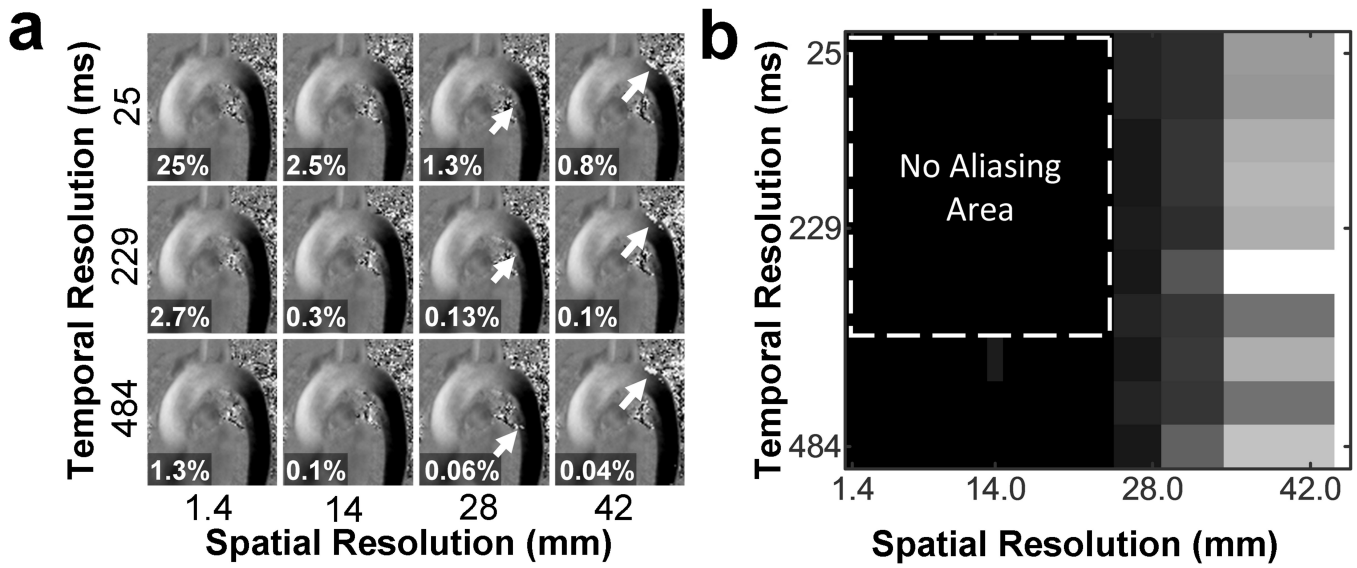

Figure 5.

Source S/I velocity images for a single volunteer (a) and measured aliasing (b) as a function of resolution for accelerated 5-point encoding. On source images, arrows point to locations of uncorrected velocity aliasing, while images are labeled with the percent increase in scan time. The no aliasing area is indicated on the measured aliasing and is bounded by a 23.8mm spatial resolution and 331ms temporal resolution. Error is significantly more dependent on spatial resolution than temporal resolution in this case.

Table 1

First moments, maximum first Moment, relative maximum first Moment and VNR comparison of 4-point reference, 4-point balanced, 5-point balanced, and 7-point referenced acquisitions. VNR values do not account for intra-voxel dephasing, which will reduce values with increasing first moment magnitude. F represents the high to low V_{enc} fraction.

Method	M_1-X	M_1-Y	M_1-Z	max(M_1)	Relative max(M_1)	Theoretical Relative VNR	Relative VNR Efficiency	Relative VNR in $V_{estimate}$
4-Point Referenced	-1,+1,-1,-1	-1,-1,+1,-1	-1,-1,-1,+1	$\frac{\pi}{2\gamma V_{enc}}$	1	1	1	NA
4-Point Balanced	-1,+1,+1,-1	-1,+1,-1,+1	-1,-1,+1,+1	$\frac{\pi}{2\sqrt{2}\gamma V_{enc}}$	≈0.7	1	1	NA
5-Point Balanced	-1,+1,+1,-1,0	-1,+1,-1,+1,0	-1,-1,+1,+1,0	$\frac{\pi}{\sqrt{3}\gamma V_{enc}}$	≈1.15	$\frac{2\sqrt{2}}{\sqrt{3}} \approx 1.6$	1.3-1.6	≈1.6
7-Point Referenced	-1,+1,-1,-1,(-1+2/F),-1,-1	-1,+1,-1,-1,-1,(-1+2/F),-1	-1,+1,-1,-1,-1,-1,(-1+2/F)	$\frac{F\pi}{2\gamma V_{enc}}$	F	F	≈0.6F	1/F